SPEED FACTORS ON LOW-VOLUME ROADS FOR HORIZONTAL CURVES AND TANGENTS

Gianluca Dell'Acqua[1], Francesca Russo[2]

Dept of Transportation Engineering, University of Naples,
Via Claudio 21, I-80125 Naples, Italy
E-mails: [1]gianluca.dellacqua@unina.it; [2]francesca.russo2@unina.it

Abstract. Many studies on driver speed behavior are found in the scientific literature today, and various researchers have addressed roadway alignment consistency for travel safety in context with current operating speeds. Experimental analysis was conducted on low-volume roads in Southern Italy without spiral transition curves between geometric tangent and circular elements on the horizontal alignment. All selected roads are located in areas with level terrain and vertical grades less than 6%. This study will illustrate a methodology, widely employed in the literature, to evaluate at each circular curve transition segment length, the applicable deceleration and acceleration rates. These results were then used to develop four equations for speed prediction models on tangents and curves. These regression equations were developed using a traditional Ordinary-least-squares method involving speed values not surveyed in transition zones. The goal of this research study is to plot continuous speed profiles to illustrate complete driver speed behavior on two-lane rural roads and to individualize critical roadway sections to improve driver safety.

Keywords: driver speed behavior, operating speed profile, roadway alignment consistency.

1. Introduction

Many studies in the scientific literature dealt with roadway safety to evaluate how the human, infrastructural and environmental factors can influence an unexpected event. Some researchers have shown how the collisions tend to occur disproportionately at certain roadway segments (Gibreel *et al.* 1999). This implies that in addition to driver error, road characteristics play a major role in collision occurrence.

The crashes were defined in the literature as the result of bad decisions by the driver made in an environment created by the engineer. International researchers (Lazda, Smirnovs 2009) have thus suggested a variety of approaches to analyze the road traffic safety level as some procedures based on the valuation of the accident rates and accident frequency.

The road traffic safety has thence become a priority field worldwide and one of the major factors describing the transport system's state with its positive and negative changes (Ratkevičiūtė *et al.* 2007).

To restrict the consequences of the roadway accidents, some experimental analyses were addressed to road safety to assess the relationships between vehicles, users and the environment. The design consistency evaluation is one of several promising tools that can be employed by roadway designers to improve roadway safety performance. Therefore, a design inconsistency in a roadway seg-

ment can surprise drivers by violating their expectancies and increases the chance of delayed response times, speed errors, and unsafe driving manoeuvres that may lead to higher collision risk.

Many researchers have verified that one of the parameters to most influence a safe driving is the speed variable. In the scientific literature some research works have dealt with speed prediction models to analyze real driver behavior.

Operating speed is defined as the speed at which drivers travel on a dry road in free flow conditions during daylight hours and is calculated using a specific percentile of speed distribution, typically the 85th. Numerous studies have shown how operating speed profiles traced on existing roadways are functional devices to check their design consistency and they can also be used to assess the impact of improvement plans for new road design projects. Design consistency, in particular, is defined as the conformity of roadway geometry and operational features to drivers' expectations.

Since 2003, the Dept of Transportation Engineering at the University of Naples has been conducting a large research program based on speed data collection on two-lane rural roads. The aim of this experimental analysis is to develop an accurate procedure to trace continuous operating speed profiles that reproduce real driver speed behavior at each roadway sections of the horizontal alignment.

2. Previous studies

Many researchers have dealt with driver speed behavior on two-lane rural roads to identify all the possible factors that may affect safety conditions during travel. These factors can be directly linked to personal choices, vehicle conditions, the infrastructure and its environmental features. In the scientific literature there are many formulations of operating speed models on tangents and curves for two – lane rural roads and there are also several analyses of driver speed behavior entering and departing circular elements to measure deceleration and acceleration rates. Operating speed models set out in the literature generally predict a mean value of V_{85} (85th percentile of speed distribution) at each geometric element, or a speed value for some roadway section.

The number of operating speed prediction models on tangents set out in the literature generally is lower than on circular elements because driver speed behavior is more complex to analyze. In fact the users have more freedom driving on tangents segments than on circular elements, and therefore the variables that can correctly explain the phenomenon are outnumber.

Polus *et al.* (2000) developed, for example, a model to predict operating speeds on tangent segments. The sites were divided into four groups based on the 28 tangent length and the preceding and following radius of the horizontal curves. Ordinary-least-squares (OLS) models were developed for each tangent group. The model has introduced one independent variable that is the average radius of horizontal curves preceding and following the tangent. The regression equation was suggested for segments having curve radius smaller than 820 ft (270.6 m) and tangent length of less than 500 ft (165 m).

Later, Fitzpatrick *et al.* (2003) collected speed and geometric data in 78 sites and speed models for five different highway classes were developed. Except for the posted speed limit and the access density, no other roadway characteristic had a relationship with the operating speeds.

Several experimental analyses also exist in the literature relating to driver behavior on the circular curve and on entering and departing circular curve. In the first case some research studies have analyzed for example the real vehicle movement trajectory according to the laws of geometry of movement and behavior of the vehicle under real traffic conditions in small radius, optimum shaping of steering path and defining of kinematic vehicle by using computer programme Dragčević *et al.* (2008). In the second case some researchers have analyzed the deceleration and acceleration motion on the transition zones. The transition zones are the regions where drivers change speed, and their extension can vary from curve to curve as will dearly be shown later. Drivers use these regions to decelerate when approaching a curve (in this case the transitions can begin before the circular element and can end within it), and to accelerate when leaving a circular curve (in this case the transitions can begin inside the circular element and end after a circular curve). Some studies have shown how acceleration and deceleration actions occurred

only on tangent segments and a constant speed was, subsequently, maintained by drivers on circular elements (Fitzpatrick, Collins 2000; Ottesen, Krammes 2000).

A complete speed – profile was studied for example by Figueroa-Medina and Tarko (2004). Using an iterative process they obtained a deceleration transition length divided as 65.5% on the approach tangent to the horizontal curve and 34.5% on the circular element, and an acceleration transition length divided as 71.6% on the departure tangent from the horizontal curve and 28.4% on the circular element. They subsequently calibrated predictive speed models on tangents and curves which are not restricted to a specific percentile, but for all percentile speeds from the 5th to the 95th in increments of five.

The aim of the research presented in this paper is the study of driver speed behavior on two lane-rural roads.

The analysis is divided into two phases: the first deals with the identification of transition regions and the assessment of deceleration/acceleration rates for each curve, while the second concerns the calibration and validation of predictive operating speed models on tangents and curves. The procedure shows driver behavior at speed transition segments and the speed value at each roadway section by using one of four developed operating speed prediction models based on geometric features.

3. Speed data collection

Speed data collection was carried in 2009 in connection with particular environmental and traffic conditions: dry roads, free flow conditions, and daylight hours. Speed measurements were conducted by using laser detectors. The detector emits and receives a pair of laser beams perpendicularly to the road's axis and it records the time, the instantaneous vehicle speed, the vehicle length and travelling direction for each passing vehicle. Instantaneous speed values were measured using the transition time of a single vehicle through two adjacent photocells inside the device.

The device was installed each section on a tripod beside the road for two to three hours on each selected roadway and it was hidden from the view of roadway users, who might have altered their speed once they had seen the device.

To investigate all selected locations, as will be further explained later, no particular day of the week was preferred for the survey because all experimental activities depended on available human, economic and material resources and on administrative decisions. The speed measurements are not error-free but the error margin never exceeded 10%. These errors can be attributed to the following factors:

– successive vehicles crossing the beam at intervals of less than 5 s;
– the presence of motorcycles (vehicles shorter than 2.5 m) and trucks (vehicles longer than 9.00 m);
– the axis of the laser beam projected toward surfaces with a low refraction rate and, sometimes, axles of vehicles not perpendicular to the axis of the roadway.

In any case vehicles, crossing the beam less than 5 s after the preceding one, were eliminated from the database to respect free flow conditions. Motorcycles and also trucks were eliminated from the database. The final sample data used to analyze driver speed behavior was made up of measurements on rural roads in free flow conditions fall within the Salerno Province network: S.P.30b (5.8 km, 43 surveyed sections), S.P.52 (3.46 km, 60 surveyed sections), S.P.312 (8.23 km, 80 surveyed sections), S.P.262 (7.12 km, 45 surveyed sections), S.S.166 (5.34 km, 99 surveyed sections) and S.S.426 (4.08 km, 84 surveyed sections).

4. Roadway features

The potential geometric elements used to study driver speed behavior were 80 tangent segments, 40 circular elements and 70 tangent-curve-tangent transitions identified during the study of deceleration and acceleration actions.

Predicted operating speed models on tangents were calibrated using 140 study sites. Speed observations on curves with a radius greater than 500 m were included in the same database because drivers' behavior is very similar to that adopted on the tangents analyzed. 100 study sites

on the other hand were used to calibrate operating speed models on circular curves with a radius of less than 500 m. At least 100 free flow speeds were measured at each site.

Table 1 shows all the features measured on selected tangents and circular segments. In particular, it can be observed the curvature change rate of an homogeneous road segment (*CCR,* gon/km) defined as the sum of the absolute values of angular changes in the horizontal alignment divided by the total length of the road section. An homogeneous roadway segment is characterized by an almost constant slope. The curvature change rate of a single curve (*CCR,* gon/km) is defined as the sum of the absolute values of angular changes in the horizontal circular element divided by the total length of the circular element. Table 2 shows the descriptive statistics of the features observed on the tangents and circular curves.

5. Data analysis

Speed measurements were taken by placing the device in a tactical location on the roadways. The laser detector was placed on the beginning section, middle section and end section of each geometric element. To study roadway

Table 1. Features on analyzed roadway segments

width	travel lanes plus shoulders, m
curve radius	radius of the horizontal curve, m
preceding curve radius	radius of the horizontal curve preceding surveyed roadway geometric element, m
preceding tangent length	length of the tangent segment preceding surveyed roadway geometric element, m
CCR of homogeneous segment	curvature change rate of an homogeneous roadway segment, gon/km
CCRs of preceding curve	curvature change rate of a single curve preceding surveyed geometric segment, gon/km
tangent and curve length	length of single geometric element, m
V_m	observed mean speed value, km/h
V_{85}	observed operating speed value, km/h

Table 2. Descriptive statistics of features on tangent and curve elements

Tangent element	Width, m	Preceding curve radius, m	*CCRs* of preceding curve, gon/km	Tangent length, m	*CCR* of homogeneous segment, gon/km	V_m, km/h	V_{85}, km/h
Mean value	6.49	184	534.29	2225.92	44.26	57.18	75.28
Max value	12.56	450	2529.21	4699.00	159.28	78.43	102.65
Min value	4.80	25	141.47	65.37	9.60	40.29	50.25
Standart deviation	1.16	101	494.26	1516.78	46.21	8.09	9.94

Circular element	Width, m	Curve radius, m	*CCR*, gon/km	*CCRs*, gon/km	Curve length, m	Preceding curve radius, m	Preceding tangent length, m	V_m, km/h	V_{85}, km/h
Mean value	6.49	170	115	593	69	1514	353	47	60
Max value	12.56	450	236	2529	218	10000	4175	72	92
Min value	4.80	25	10	141	22	20	2	25	31
Standart deviation	1.16	106	81	506	38	3240	684	12	15

users' approach curve and departure curve movements, the laser was also placed in three different positions at the beginning and end segments of the circular element: the first changes from 30 m to 50 m, the second changes from 80 m to 120 m and the third changes from 140 m to 200 m.

5.1. Acceleration and deceleration rates

V_{85} profiles were designed for two travelling directions of all selected roadways, and a careful analysis was carried out to identify the real transition zone occupied by drivers to decelerate approaching a curve and to accelerate leaving the curve for each circular element.

To detect the deceleration transition zone at each curve the furthermost surveyed location from the beginning section of the curve where the user starts to decelerate and the final location where deceleration terminates were identified. To detect the acceleration transition zone at each curve the furthermost surveyed location from the end section of the curve where the user stops accelerating and the initial location where acceleration starts were observed.

These transition segments can enclose a portion of circular horizontal curve and near-tangent because there are no spiral transitions on the roadways analyzed.

Careful study of transitions length has, in this case, returned a max transition segment on a tangent element of 200 m from PC (point of curvature) or PT (point of tangent) sections. This value, according to the operating speed profiles, was never exceeded by drivers to adjust their speeds in order to apply the desired acceleration or deceleration rate.

Fig. 1 summarizes all the driver speed behavior types decelerating and accelerating circular curves respectively.

It can be observed in particular as the max surveyed transition length appears in the first image where deceleration transition length on approaching tangent is equal to 194.55 m from PC section. On the x-axis are the distances, in m, from the middle section (MC) of the curve, fixed positive on approaching curve and negative on departing curve, and on the y-axis there is the observed V_{85} in km/h. The operating speed profile in Fig. 1 illustrates the PC, PT and MC positions, the direction of travel (by arrow), distance L_d (segment length used by drivers to decelerate approaching curve) and distance L_a (segment length used by drivers to accelerate departing curve).

The deceleration rates ($d_{m_{VES}}$) and acceleration rates ($a_{m_{VES}}$) were estimated using a methodology commonly employed in the literature.

This methodology is based on the operating speed profile; the rates are assessed using the following procedure:

- $d_{m_{VES}}$ – deceleration rate, in m/s², is measured a long distance L_d, in m, by using two operating speed values. The first one (V_1, km/h), where the max V_{85} is reached on approaching a curve, can be located at no further than 200 m upstream of the PC section and it can also correspond with the PC section if the drivers occupy the total curve length in deceleration. The second one (V_2, km/h) is observed on the circular curve where the min V_{85} is reached:

$$d_{m_{VES}} = \frac{V_1^2 - V_2^2}{2 \times L_d} \times 3.6^{-2}, \qquad (1)$$

- $a_{m_{VES}}$ – acceleration rate, in m/s², is estimated a long distance L_a, in m, by using two operating speed values. The first one (V_1, km/h), where the max V_{85} is reached on the departure curve can be located at the most 200 m downstream of the PT section and it can also correspond with the PT section if the drivers occupy the total curve length in acceleration. The second one (V_2, km/h) is observed on the circular curve where the min V_{85} is reached

$$a_{m_{V85}} = \left(\frac{V_1^2 - V_2^2}{2 \times L_a} \right) \times 3.6^{-2}, \qquad (2)$$

36 and 34 sites were employed to assess acceleration and deceleration rates as shown in Table 3.

The parameters estimated for each site (tangent-curve-tangent transition) are shown in Table 3. In particular, the meaning of the parameters shown in Table 4 is as follows: L_d – deceleration transition length ($L_d = t_d + c_d$), m; t_d – part of distance L_d located on the approach tangent, m and %; c_d – part of distance L_d on the horizontal curve, m and %; L_a – acceleration transition length ($L_a = t_a + c_a$), m; t_a – part of distance L_a located on the departure tangent, m and %; c_a – part of distance L_a on the horizontal curve, m and %.

T-tests were, subsequently, performed to assess if:

1) the mean value of acceleration rates, shown in Table 3, equal to 0.68 m/s² and measured using 34 study sites, can be considered statistically equal to the current rate of 0.80 m/s² adopted in the Italian Standard Design to trace a speed profile (H_0: $a_{m_{VES}}$ = 0.80; H_1: $a_{m_{VES}}$ ≠ 0.80) at significant level equal to 5%;

2) the mean value of deceleration rates equal to 0.70 m/s², measured using 36 study sites, can be considered statistically equal to the current rate of 0.80 m/s² adopted in the Italian Standard Design to trace a speed profile (H_0: $d_{m_{VES}}$ = 0.80; H_1: $d_{m_{VES}}$ ≠ 0.80) at a significant level equal to 5%.

A first application of the t-test did not rejected the H_0 hypothesis: in fact it can be observed a mean difference of rates of 0.12 ms⁻², standart deviation of 34 study sites of 0.369 ms⁻², mean standart error of 0.063 ms⁻² and t_{calc} equal to –1.83 with p-value (2-tailed) equal to 0.076. The second application of the *t*-test did not reject the H_0 hypothesis: in fact it can be observed a mean difference of 0.10 ms⁻², a standart deviation of 36 study sites of 0.44 ms⁻², a mean standart error equal to 0.074 ms⁻², t_{calc} equal to –1.31 with the p-value (2-tailed) equal to 0.20.

Analyzing the standard deviation (σ_d) and mean (μ_d) of the 36 sample values of deceleration rates, using the

"3σ" method, no rate was rejected. It was noted how 81% of measurements fall within the range μ ± σ = 0.71 m/s^2 ± 0.45 m/s^2 = 0.26–1.16 m/s^2, and how all the values fall within the range μ ± 3s. Then, analyzing the standard deviation (σ$_a$) and mean (μ$_a$) of 34 values for acceleration rates, no rate was rejected. It was noted how 75% of measurements fall within the range μ ± σ = 0.60 m/s^2 ± 0.37 m/s^2 = 0.23–0.97 m/s^2, and how all the values fall within the range μ ± 3σ. The deceleration and acceleration rates, calculated assuming a uniform motion along the transition distances L_d and L_a, can be used to develop an easy and real operating speed – profile model.

5.2. Operating speed prediction models

Four predictive operating speed models were developed for analyzed roadways: two models on tangents and two models on the circular curves. Two models on tangents were associated with the segment length: the first one can be applied on the tangents with a length of less than 500 m and the second one on tangents with a length greater than 500 m.

The models were performed applying the following restrictions:
 – no section may outdistance the intersections by less than 50 m;
 – no sections fall in the identified transition segments;
 – all spots on the circular elements with a radius greater than 500 m are included in the data base.

Two operating speed models on the circular elements were associated to a mean *CCR* value of the roadway segment to which the curve belonged: the first one can be applied on the curves with a *CCR* value of less than 240 gon/km and the second one with a *CCR* value greater than 240 gon/km.

All parameters included in the models are significant with a 95% confidence level.

The best specification of the OLS of operating speeds on tangents, in km/h, with a length greater than 500 m was worked out from 105 study sites; the equation – form is the following:

$$V_{85T} = 66.94 + 0.00475 \times L_T + 0.0137 \times R_{PC}^{1.5} - 0.29 \times R_{PC} +$$
$$0.3019 \times V_{85PC} - 5.24 \times INT + 0.0594 \times W^2 - 0.579 \times RES,$$

(3)

where L_T – the total tangent length, m; R_{PC} – the radius of the preceding curve, m; V_{85PC} – the operating speed in the middle section of the preceding curve, km/h; *INT* – the intersection indicator equal to 1 if intersection is located 150 m before or after the surveyed location, 0 otherwise; *W* – travel lanes plus shoulders, m; *RES* – the number of residential drive-ways per km.

The adjusted coefficient of determination (ρ^2) of the model is equal to 71.7%.

The best specification of the OLS model for operating speeds on the tangents with a length of less than 500 m,
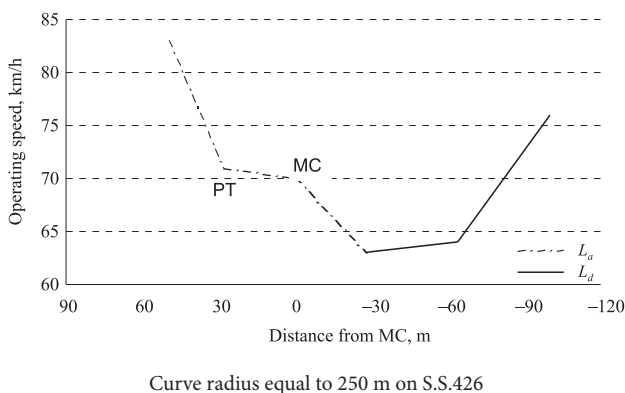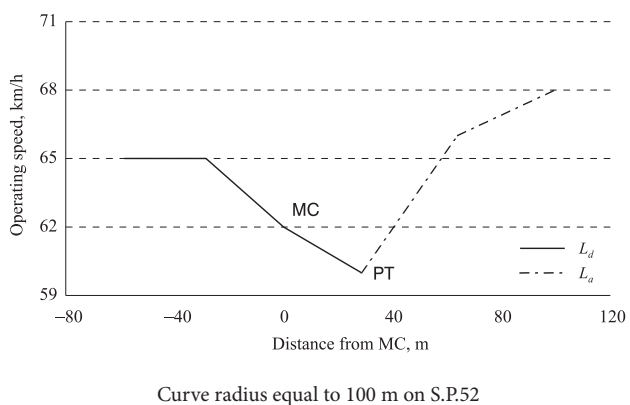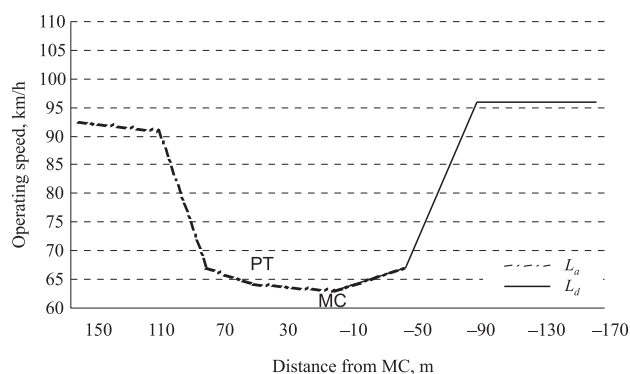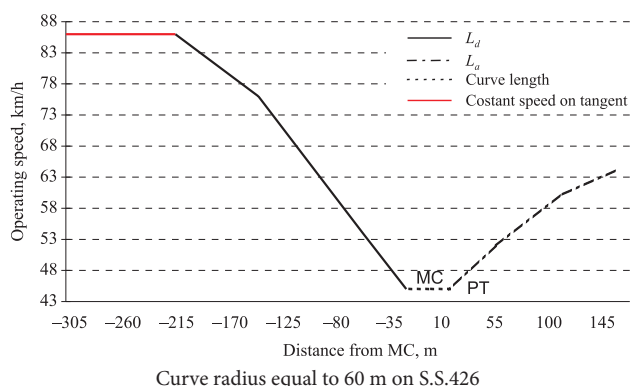
Fig. 1. Example of transitions for different curves

Table 3. $d_{m_{VES}}$, $a_{m_{VES}}$ values and transition length for surveyed sites

Site	Curve radius, m	$d_{m_{VES}}$, ms^{-2}	$a_{m_{VES}}$, ms^{-2}	L_d, m	L_a, m	t_d, m	c_d, m	t_a, m	c_a, m	t_d, %	c_d, %	t_a, %	c_a, %
1	100	0.79	0.31	115.5	191.0	115.5	0	113.5	77.5	100.00	–	59.42	40.58
2	100	–	1.05	–	165.5	–	–	128	37.5	–	–	77.34	22.66
3	280	0.29	–	122.0	–	0	122	–	–	–	100.00	–	–
4	280	0.27	0.60	75.0	172.0	75	0	50	122	100.00	0.00	29.07	70.93
5	200	–	–	–	–	–	–	–	–	–	–	–	–
6	200	0.82	–	206.0	–	131	75	–	–	63.59	36.41	–	–
7	145	0.32	0.57	325.0	36.5	180	145	36.5	0	55.38	44.62	100.00	0.00
8	145	0.39	0.46	72.5	252.5	0	72.5	180	72.5	0.00	100.00	71.29	28.71
9	200	0.32	–	173.0	–	173	0	–	–	100.00	0.00	–	–
10	200	0.46	0.62	32.0	32.0	0	32	0	32	0.00	100.00	0.00	100.00
11	50	–	0.33	–	411.5	–	–	390	21.5	–	–	94.78	5.22
12	300	1.66	–	63.0	0.0	0	63	–	–	0.00	100.00	–	–
13	100	0.55	0.42	86.0	99.0	69	17	82	17	80.23	19.77	82.83	17.17
14	100	0.38	0.45	58.0	155.0	41	17	17	138	70.69	29.31	10.97	89.03
15	110	1.42	0.93	45.0	52.5	0	45	0	52.5	0.00	100.00	0.00	100.00
16	110	1.04	0.58	52.5	45.0	0	52.5	0	45	0.00	100.00	0.00	100.00
17	50	0.31	0.40	433.0	196.5	390	43	196.5	0	90.07	9.93	100.00	0.00
18	100	0.42	0.71	71.0	57.0	71	0	0	57	100.00	0.00	0.00	100.00
19	100	0.22	0.56	87.0	71.0	30	57	71	0	34.48	65.52	100.00	0.00
20	90	0.68	1.18	22.8	77.3	22.8	0	44.2	33.1	100.00	0.00	57.20	42.79
21	90	0.47	–	88.6	–	44.2	44.4	–	–	49.86	50.14	–	–
22	60	0.50	0.53	175.5	286.6	138.9	36.6	250	36.6	79.14	20.86	87.23	12.77
23	60	0.72	0.46	286.6	175.5	250	36.6	175.5	0	87.23	12.77	100.03	0.00
24	250	1.88	0.58	67.8	162.2	27.8	40.0	122	40	41.02	59.05	75.21	24.66
25	250	–	1.26	0.0	84.0	–	–	83.98	0	–	–	100.00	0.00
26	400	0.42	0.27	409.2	290.8	301	108.2	290.8	0	73.55	26.44	100.00	0.00
27	400	–	0.28	–	355	–	–	301	54	–	–	84.79	15.21
28	240	0.44	1.35	199.7	59.7	140	59.7	0	59.7	70.09	29.89	0.00	100.0
29	240	1.24	0.27	97	303.0	37.6	59.4	243	60	38.66	61.07	80.20	19.80
30	150	0.38	0.62	81.3	103.0	0	81.3	103	0	0.00	99.99	100.00	0.00
31	150	0.77	1.68	40.0	41.6	40	0	0	41.6	100.00	0.00	0.00	100.0
32	250	0.82	0.79	70.2	28.0	42.2	28	0	28	60.11	39.89	0.00	100.00
33	250	0.97	1.45	71.8	77.7	72	0	21.7	56	100.00	0.00	27.93	72.07
34	100	1.89	–	18.7	–	0	18.7	–	–	0.00	100.00	–	–
35	100	1.03	0.71	63.4	117.0	63.4	0	101	16	100.0	0.00	86.32	13.68
36	100	0.61	0.71	117.9	16.7	117.9	0	0	16.7	100.0	0.00	0.00	100.0
37	100	0.75	1.17	45.3	28.9	45	0	0	28.9	100.0	0.00	0.00	100.00
38	100	0.26	0.46	46.7	92.0	47	0	34	58	100.0	0.00	36.96	63.04
39	180	0.39	0.29	45.8	45.8	0	45.8	0	45.8	0.00	100.00	0.00	100.00
40	180	0.65	0.46	128.8	26.7	128.8	0	0	26.7	100.00	0.00	0.00	100.00
41	70	0.79	–	55.2	–	28.2	27	–	–	51.09	48.91	–	–
42	70	–	0.77	–	110.0	–	–	82	28	–	–	74.55	25.45
		mean observed value								mean observed value, %			
		0.70	0.68	115	130					60.00	40.00	51.00	49.00

in km/h was developed from 35 study sites. The equation form is the following:

$$V_{85T} = 75.18 + 0.000337 \times R_{PC}^2 - 0.123 \times R_{PC} +$$
$$0.01697 \times D - 3.48 \times INT + 0.042 \times W^2 - 0.471 \times RES, \quad (4)$$

where D – distance of the surveyed point from the end section of the preceding horizontal curve, m.

The adjusted coefficient for the determination (ρ^2) of this speed model is equal to 78.3%.

The best specification of the OLS model for operating speeds on horizontal curves with a mean *CCR* value of less than 240 gon/km, in km/h, was developed using 48 study sites.

The equation form is following:

$$V_{85C} = 68.22 + 2.81 \times W - 0.035 CCR_s + 0.00001 \times$$
$$CCR_s^2 - 0.0017 \times L_s - 0.56 \times RES - 1.84 \times INT +$$
$$0.00157 \times L_{PT} - 0.047 \times CCR, \quad (5)$$

where CCR_S – curvature change rate of a single curve, gon/km; L_s – the length of single circular element, m; L_{PT} – the preceding tangent length, m.

The adjusted coefficient of determination (ρ^2) of this speed model is equal to 88.6%.

The best specification of the OLS model for operating speeds on horizontal curves with a mean *CCR* value greater than 240 gon/km, in km/h, was developed from 52 study sites; the equation is the following:

$$V_{85C} = 61.59 + 0.022 W^2 - 0.015 \times CCR_s + 0.00001 \times$$
$$CCR_s^2 + 0.0001 \times L_s^2 - 0.018 \times RES - 1.72 \times INT. \quad (6)$$

The adjusted coefficient of determination (ρ^2) of this speed model is equal to 81.4%.

5.3. Validation procedure of the prediction models

Four speed prediction models were then tested. The methodology, described below, was applied on two-lane rural roads that were not included in the data base used to calibrate operating speed prediction models.

The roadways used for the validation procedure were S.P. 135 and S.S. 103 located in the Province of Salerno in Southern of Italy. These roads reflect the features of those adopted in the calibration phase. Speed data were collected in free–flow conditions during daylight hours and in dry road conditions.

The validation procedure is to estimate some synthetic statistical parameters:

– Mean error – mean value of speed differences (D_i) assessed at each study site between observed operating speed value and predicted operating speed value;

– *MAD (Mean Absolute Deviation)* – constant value equal to the sum of the absolute values D_i divided by the number (n) of study sites:

$$MAD = \sum_{i=1}^{n} \frac{|D_i|}{n}; \quad (7)$$

– *MSE (Mean Squared Error)* – constant value equal to the sum of D_i^2 values divided by the number of sites:

$$MSE = \sum_{i=1}^{n} \frac{D_i^2}{n}; \quad (8)$$

– *I* – constant value equal to the square root of MSE divided by the mean predictive operating speed value:

$$I = \frac{\sqrt{MSE}}{\sum_{1}^{n} \frac{V_{(operating\ speed\ model)}}{n}}. \quad (9)$$

The validation procedure for the operating speed model on a tangent with a length greater than 500 m involved 12 study sites, 8 of which were on S.P.135 and 4 on S.S.103, while for the tangents with a length of less than 500 m 7 study sites on S.P.135 were involved. The validation procedure for the operating speed model on the horizontal curves with a *CCR* of less than 240 gon/km involved 22 study sites, 8 of which were placed on S.P.135 and 14 on the S.S.103, while for horizontal curves with a *CCR* longer than 240 gon/km, 34 study sites on S.S.103 were taken into consideration. Table 4 shows the values returned by the analysis of summarizing statistical parameters.

Table 5 shows the range of residuals returned by difference between observed and predicted operating speed for each of four models, where μ is the mean value and σ is the standard deviation of this difference.

Table 4. Parameters returned by validation procedure

Prediction model	Mean error (μ)	MAD	MSE	I
Tangent length > 500 m	–3.49	11.0	166.3	0.15
Tangent length < 500 m	7.38	8.4	119.5	0.13
Curves with *CCR* > 240 gon/km	–2.20	5.8	48.6	0.11
Curves with *CCR* < 240 gon/km	1.90	11.3	221.0	0.18

Table 5. Range of residuals for prediction models

Prediction model	Residuals range	
Tangent length > 500 m	[μ – 2σ ; μ + 2σ]	[–29.29 km/h; 22.30 km/h]
Tangent length < 500 m	[μ – 2σ ; μ + 2σ]	[–14.48 km/h; 29.25 km/h]
Curves with *CCR* > 240 gon/km	[μ – 2σ ; m + 3σ]	[–16.10 km/h; 18.70 km/h]
Curves with *CCR* < 240 gon/km	[μ – 2σ ; μ + 3σ]	[–27.83 km/h; 38.92 km/h]

In particular, it was noted how for all the operating speed prediction models more than 50% of residuals fall within the range $\mu \pm \sigma$, where the max value of the residual is of less than 15 km/h. It can be concluded that speed prediction models are statistically significant because the residuals fall within a limited range around the mean. This was confirmed by the low value of *MAD* and *I* indicators.

6. Results and operating speed model procedure

The study of driver speed behavior on two-lane rural roads was divided into two phases for the purposes of this study: the first phase dealt with the identification of transition zones and the estimation of deceleration/acceleration rates at each circular element, while the second one dealt with the calibration and validation of operating speed prediction models on tangents and curves to trace a complete operating speed profile.

The study of transitions relied on a methodology based on the operating speed profiles. The mean value of the deceleration transition length (L_d) and acceleration transition segment (L_a) for two-lane rural roads without spiral transitions between tangents and circular elements, located in the Salerno Province (Italy), was shown in Table 3. It shows how the mean value L_d is equal to 115 m and the mean value L_a is equal to 130 m. In particular L_d is divided thus: 60% on the approach tangent at the horizontal curve from the PC section and 40% on the circular element, while L_a is divided as follows: 51% on the departure tangent from the PT section and 49% on the circular curve.

In particular, it can be seen how the mean deceleration rate, used by drivers entering circular elements, is equal to 0.70 m/s^2 and it is not statistically different from the current rate adopted in the Italian Standard Design, equal to 0.80 m/s^2, like the mean acceleration rate equal to 0.68 m/s^2 adopted by drivers departing curves.

Therefore, once the transition segments were identified at each circular element, operating speed prediction models on tangents and horizontal curves can be calibrated using the remainder of the collected speed values.

Two operating speed models were produced on the tangents: the first one related to lengths greater than 500 m and the second one connected to lengths of less than 500 m. Two operating speed models were also produced on the circular curves: the first related to a mean *CCR* value of an homogeneous road segment greater than 240 gon/km and the second related to a *CCR* value of less than 240 gon/km.

Four models have an adjusted coefficient of determination (ρ^2) greater than 70% and they offer the operating speed value at each point on the horizontal alignment as the roadway features vary.

All models were then validated by comparing predicted speed values with observed speed values not included in the calibration phase. This procedure analyzes some summarizing statistical parameters that confirm the correctness of the regression equations.

A complete operating speed profile can finally be traced on two-lane rural roads by using the following steps:

a) Placing L_d and L_a distances for each curve according to the results of the data analysis:
- 60% of L_d occurs on the approach tangent from the beginning section of a circular element;
- 40% of L_d occurs on the circular element from its beginning section;
- 51% of L_a occurs on the departure tangent from the end section of a circular element;
- 49% of L_a occurs on a circular element from its end section.

b) Measuring the operating speed value at initial and final section of L_d and L_a by one of four developed models;

c) Measuring the real deceleration length L_d and acceleration length L_a, in m, for each circular element, assuming a uniform motion along the transition distance, applying the following Eqs (10) and (11):

$$L_d = \left[\frac{V^2_{85_{approach\_tangent}} - V^2_{85_{curve}}}{2 \times 0.70} \right] \times 3.6^{-2}, \quad (10)$$

$$L_a = \left[\frac{V^2_{85_{departure\_tangent}} - V^2_{85_{curve}}}{2 \times 0.68} \right] \times 3.6^{-2}, \quad (11)$$

where $V_{85approach\_tangent}$: predicted operating speed value, km/h, observed on the approach tangent and assessed by one of two developed models according to length. The value to use in the formulation is the max value observed at no more than 200 m upstream of the PC section, as shown in more detail above; $V_{85curve}$: predicted operating speed value, km/h, observed on a circular curve and assessed by one of two models according to the *CCR* value; the value to use in the formulation is the min V_{85}; 0.70: mean deceleration rate, m/s^2, employed on the analyzed roads by drivers entering circular elements; $V_{85departure\_tangent}$: predicted operating speed value, in km/h, observed on departure tangents and assessed by one of two models according to length; the value to use in the formulation is the max value observed at a max 200 m downstream of the PT section; $V_{85curve}$: predicted operating speed value, in km/h, observed on circular curves and assessed using one of two models depending on the *CCR* value; the value to use in the formulation is the min V_{85}; 0.68: mean acceleration rate, in m/s^2, employed on the analyzed roads by drivers leaving circular elements.

Fig. 2 shows an example of the continuous speed profiles by using operating speed prediction models presented in this paper according to the increase of km. In particular it can be observed the direction of travel (by arrow), on the *x* axis the distances, in m, and on the *y* axis the values of the observed and predicted V_{85}, in km/h.
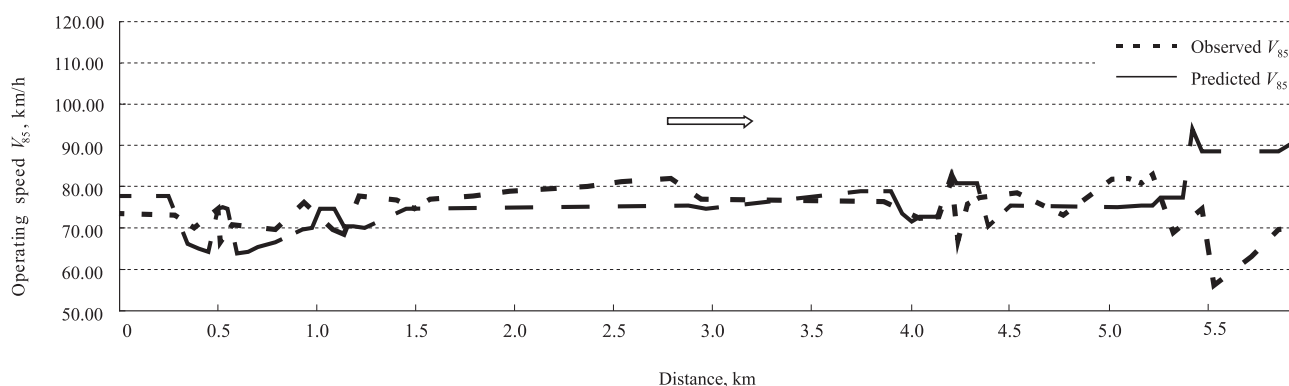
Fig. 2. Operating speed profiles on S.P.135 according to the increase of km

7. Conclusions

Once real deceleration and acceleration transition length are known, a continuous operating speed profile can be designed for the total length of the roads. Speed value at each roadway point will determine using one of four operating speed prediction models depending on the geometric features present.

In cases where the length of the curve was smaller than the combined length of the deceleration and the acceleration transition sections inside the curve, the drivers don't reach a constant speed on the curve. If the transition sections overlapped inside the curve, the smallest speed reduction due to the deceleration or the acceleration at a specific spot was selected.

This procedure can be also used in carrying out safety analyses of existing two-lane rural roads in Italy. In fact, assessing the real difference between the operating speed value using models and the speed value put forward by the Italian standard, it is possible to act on the horizontal-vertical alignment to improve the roadway design and increase safety for users. Future development of research addresses the investigation of differences in the driver's behavior on the roadways with and without spiral transitions between tangent and circular elements.

References

Dragčević, V.; Korlaet, Z.; Stančerić, I. 2008. Methods for Setting Road Vehicle Movement Trajectories, *The Baltic Journal of Road and Bridge Engineering* 3(2): 57–64.
doi:10.3846/1822-427X.2008.3.57-64

Figueroa-Medina, A.; Tarko, A. P. 2004. *Reconciling Speed Limits with Design Speeds*. Final Report FHWA/IN/JTRP-2004/26, Purdue University ‒ Joint Transportation Research Program Project No. C-36-10G File No. 8-3-7 SPR- 2661, Purdue University West Lafayette, IN 47907.

Fitzpatrick, K.; Carlson, P.; Brewer, M.; Wooldridge, M.; Miaou, S. 2003. *Design Speed, Operating Speed and Posted Speed Practices* [cited 9 September, 2009]. Available from Internet: <http://onlinepubs.trb.org/onlinepubs/nchrp_wrpt_504.pdf>.

Fitzpatrick, K.; Collins, J. M. 2000. Speed Profile Model for Two-Lane Rural Highways, *Transportation Research Record* 1737: 42–49. doi:10.3141/1737-06
doi:10.3141/1737-06

Gibreel, G. M.; Easa, S. M.; Hassan, Y.; El-Dimeery, I. A. 1999. State of the Art of Highway Geometric Design Consistency, *Journal of Transportation Engineering* 125(4): 305–313.
doi:10.1061/(ASCE)0733947X(1999)125:4(305)

Lazda, Z.; Smirnovs, J. 2009. Evaluation of Road Traffic Safety Level in the State Main Road Network of Latvia, *The Baltic Journal of Road and Bridge Engineering* 4(4): 156–160.
doi:10.3846/1822-427X.2009.4.156-160

Ottesen, J. L.; Krammes., R. A. 2000. Speed Profile Model for Design-Consistency Evaluation Procedure in the United States, *Transportation Research Record* 1701: 76–85.
doi:10.3141/1701-10

Polus, A.; Fitzpatrick, K.; Fambro, D. B. 2000. Predicting Operating Speeds on Tangent Sections of Two-Lane Rural Highways, *Transportation Research Record* 1737: 50–57.
doi:10.3141/1737-07

Ratkevičiūtė, K.; Čygas, D.; Laurinavičius, A.; Mačiulis, A. 2007. Analysis and Evaluation of the Efficiency of Road Safety Measures Applied to Lithuanian Roads, *The Baltic Journal of Road and Bridge Engineering* 2(2): 81–87.